Murine coronavirus infection activates AhR in an IDO1-independent manner contributing to cytokine modulation and pro-viral TiPARP expression

Matthew E. Grunewald[a], Mohamed G. Shaban[a], Samantha R. Mackin[a], Anthony R. Fehr[b], and Stanley Perlman[a]#

[a]Department of Microbiology and Immunology, University of Iowa, Iowa City, Iowa, USA

[b]Department of Molecular Biosciences, University of Kansas, Lawrence, Kansas, USA

Running Head: Coronavirus infection activates AhR

#Address correspondence to Stanley Perlman, Department of Microbiology and Immunology, University of Iowa, 51 Newton Road, Iowa City, IA 52242, tele: 319-335-8549; email: stanley-perlman@uiowa.edu

Word count:

Abstract: 222. Importance: 117. Text: 4115

Abstract

The aryl hydrocarbon receptor (AhR) is a cytoplasmic receptor/transcription factor that modulates several cellular and immunological processes following activation by pathogen-associated stimuli, though its role during virus infection is largely unknown. Here, we show that AhR is activated in cells infected with mouse hepatitis virus (MHV), a coronavirus, and contributes to the upregulation of downstream effector TCDD-inducible poly(ADP-ribose) polymerase (TiPARP) during infection. Knockdown of TiPARP reduced viral replication and increased interferon expression, suggesting that TiPARP functions in a pro-viral manner during MHV infection. We also show that MHV replication induced expression of other genes known to be downstream of AhR in macrophages and dendritic cells and in livers of infected mice. Further, we found that chemically inhibiting or activating AhR reciprocally modulated expression levels of cytokines induced by infection, specifically IL-1β, IL-10, and TNFα, consistent with a role for AhR activation in the host response to MHV infection. Furthermore, while indoleamine 2,3-dioxygenase (IDO1) drives AhR activation in other settings, MHV infection induced equal expression of downstream genes in WT and IDO1$^{-/-}$ macrophages, suggesting an alternative pathway of AhR activation. In summary, we show that coronaviruses elicit AhR activation by an IDO1-independent pathway, contributing to upregulation of downstream effectors including the pro-viral factor, TiPARP, and to modulation of cytokine gene expression and identify a previously unappreciated role for AhR signaling in CoV pathogenesis.

Importance

Coronaviruses are a family of positive-sense RNA viruses with human and agricultural significance. Characterizing the mechanisms by which coronavirus infection dictates pathogenesis or counters the host immune response would provide targets for the development of therapeutics. Here, we show that the aryl hydrocarbon receptor (AhR) is activated in cells infected with a prototypic coronavirus, mouse hepatitis virus (MHV), resulting in expression of several effector genes. AhR is important for modulation of the host immune response to MHV and plays a role in the expression of TiPARP, which we show is required for maximal viral replication. Taken together, our findings highlight a previously unidentified role for AhR in regulating coronavirus replication and the immune response to the virus.

Introduction

Coronaviruses (CoVs) are a group of positive-sense single-stranded RNA viruses responsible for agricultural and human disease with high economic burden and outbreak potential. Understanding the pathways driving CoV replication and pathogenesis is crucial to combat CoVs with high mortality such as severe acute respiratory syndrome (SARS) and Middle East respiratory syndrome (MERS) CoVs. Mouse hepatitis virus (MHV), a prototypic CoV, causes hepatitis and/or encephalitis depending on the strain. Previous studies have detailed many of the cellular pathways critical for or elicited by MHV infection (1, 2). Several antiviral mechanisms are induced by MHV infection, but MHV encodes proteins that counter these host processes. For instance, interferons (IFNs), especially type 1 IFNs (IFN-I), are vital to limiting MHV infection in mice (3, 4), but IFN-I production and signaling are inhibited during MHV infection in multiple cell types (5-7). MHV also inhibits the functions of downstream IFN-stimulated genes (ISGs). For example, the MHV

macrodomain, a virally encoded ADP-ribosylhydrolase, reverses cellular ADP-ribosylation by IFN-I-induced poly(ADP-ribose) polymerases (PARPs) that limit viral replication (8, 9).

The aryl hydrocarbon receptor (AhR) is a receptor/transcription factor that has been shown to direct multiple host responses. While initially believed to operate only in the context of the cellular response to toxins, AhR is now recognized as a significant regulator of the host immune response as well. AhR in the cytosol is activated by binding ligands which are exogenous, such as the toxin 2,3,7,8-tetrachlorodibenzodioxin (TCDD), or endogenous, such as cellular metabolites (Fig. 1). This triggers AhR translocation to the nucleus, where AhR complexes with AhR nuclear translocator (ARNT) or other binding partners to induce expression of several different proteins (downstream effectors) responsible for degrading the xenobiotic agent and for limiting potential cellular damage. Upregulated genes include cytochrome P450 enzymes (CYPs) that catabolize the exotoxin, negatively regulating AhR activation by depleting AhR ligands (10). Another inhibitory protein, the AhR repressor (AhRR), is also upregulated and competes with ARNT for AhR dimerization in the nucleus (11). PARP7, also known as TCDD-inducible PARP (TiPARP), is highly induced by AhR activation as well, indicating a relationship to cellular ADP-ribosylation. TiPARP is responsible for mitigating the pathology after TCDD administration to mice at least in part due to feedback inhibition of AhR (12).

In the context of the immune response, endogenous metabolites are likely the primary ligands that drive AhR activation. The prototypical endogenous ligand is kynurenine, a tryptophan catabolite produced by indoleamine 2,3-dioxygenase 1 or 2 (IDO1 or IDO2) in immune cells or tryptophan 2,3-dioxygenase (TDO, encoded by the *TDO2* gene) in the liver (13, 14). IDO1, the best characterized of these enzymes, is induced by inflammatory factors such as IFN-I or II, TGFβ, and IL-6 (15). AhR also activates IDO1 expression and enhances its activity through multiple

pathways (16), and the resulting IDO1-AhR-IDO1 positive feedback loop prolongs effects of AhR activation (17, 18). Though kynurenine is believed to be the predominant derivative of tryptophan that drives AhR activation, multiple other degradation products of tryptophan or other biomolecules are synthesized independent of IDO1/2 or TDO or can be sourced from the gut microflora, diet, or even UV-mediated photo-oxidation (19). Prostaglandins, cAMP, and oxidative species may also activate AhR though with unknown physiologic or pathologic significance (20-22).

Many studies have demonstrated that AhR activation during immunostimulation and inflammation generally exerts a immunosuppressive effect via multiple mechanisms (23). AhR activation by chemical agonists has been shown to influence the differentiation (24-28) and cytokine/chemokine production (25, 26, 29-32) of T cells, dendritic cells, and macrophages. AhR has also been shown to bind to and modulate the transcription specificity of NF-κB in multiple experimental settings, which could contribute to cytokine modulation (30, 33-35). Other studies have shown that AhR activation in immune cells is driven by IDO1, and the resulting IDO1-AhR-IDO1 positive feedback loop helps to establish immunotolerance (18, 36, 37). In contrast, less is known about the role of AhR during virus infection. While previous work has explored pathways affected by AhR activation during in influenza A virus (IAV), herpes simplex virus (HSV), hepatitis C virus (HCV), and Epstein-Barr virus (EBV) infection (38-41), the virological impact of AhR is still largely uncharacterized. Here, we show that CoV replication in macrophages results in AhR activation in an IDO1-independent manner, leading to increased expression of several downstream effectors and to modulation of the cytokine response. We also show that TiPARP, induced by AhR, is a pro-viral factor in CoV-infected cells.

Results

MHV-A59 infection induces TiPARP expression through IFN-I-dependent and -independent mechanisms.

Infection of bone-marrow derived macrophages (BMDMs) with the neurotropic JHM strain of MHV (MHV-JHM) results in increased expression of several IFN-I-inducible PARPs (PARPs 7, 9-12 and 14) (8). However, PARP7 (TiPARP) was also induced during MHV-JHM infection of IFNAR$^{-/-}$ BMDMs, suggesting that other factors besides IFN-I mediate TiPARP upregulation during infection (8). To expand on these results, we infected Delayed Brain Tumor (DBT) astrocytoma cells (Fig. 2A) or 17Cl-1 fibroblast-like cells (Fig. 2B), both of which minimally produce IFN during MHV infection (6, 7), with the A59 strain of MHV (MHV-A59). We used MHV-A59 because it replicates to higher titers than MHV-JHM *in vitro* (42). Upregulation of most PARPs, including PARPs 9, 11, 12, and 14, was lost or attenuated in these cell lines during infection, contrasting with the robust PARP upregulation profile seen in MHV-A59-infected wild type (WT) BMDMs (Fig. 2C). Despite the diminished expression of many IFN-dependent PARPs, TiPARP was highly upregulated following MHV-A59 infection in all three cell types, suggesting a conserved mechanism of induction. Furthermore, induction of TiPARP in IFNAR$^{-/-}$ BMDMs was conserved after infection with MHV-A59, consistent with previous findings with MHV-JHM (Fig. 2D). Although not further studied here, PARP13 was also upregulated in infected IFNAR$^{-/-}$ cells. Overall, these results indicate that TiPARP is upregulated by another pathway during infection in the absence of IFN-I signaling.

TiPARP knockdown restricts MHV-A59 replication.

We previously noted that viral genomic RNA (gRNA) levels during MHV-JHM infection were reduced in BMDMs treated with siRNA directed toward TiPARP (8). To confirm this

phenotype, we treated BMDMs with TiPARP-specific siRNA prior to infection with MHV-A59 at low (0.1 PFU/cell) and high (5 PFU/cell) multiplicities of infections (MOIs) and measured replication by quantification of viral genomic content and infectious virus (Fig. 3). At low MOI at 12 hours post infection (hpi), TiPARP knockdown decreased viral gRNA levels (Fig. 3A) and titers (Fig. 3B), though the former only trended towards statistical significance. MHV infection at MOI of 5 PFU/cell showed significantly decreased gRNA levels and virus titers in TiPARP knockdown cells (Fig. 3C & D), indicating a role for TiPARP in facilitating MHV-A59 infection. These differences in gRNA and virus titers even persisted at later time points p.i. when cell viability was decreased, resulting in decreased infectious virus titers. Furthermore, while IFNα4 and IFNβ mRNA levels were unaffected by TiPARP deficiency at low or high MOI at 6 or 12 hpi, they were increased at 18 and 22 hpi (Fig. 3A & C). Together, our results suggest that TiPARP augments MHV replication throughout infection and negatively regulates IFN-I expression during later stages of infection.

MHV-A59 replication *in vitro* and *in vivo* induces expression of effector genes downstream of AhR activation.

Because expression of TiPARP is well established to be induced by ligand-activated AhR (43), we hypothesized that MHV-A59 infection resulted in AhR activation. To assess AhR activation during MHV-A59 infection in BMDMs at multiple time points, we quantified mRNA expression of known effectors downstream of AhR, including CYP1A1, CYP1A2, CYP1B1, TiPARP, and AhRR (Fig. 1). We also analyzed gene expression of AhR itself and of AhR ligand-producing enzymes IDO1, IDO2, and TDO as IDO1 gene expression can also be induced by AhR activation. We found that, while CYP1A1, CYP1A2, IDO2, and TDO2 mRNA were undetectable at all time points, CYP1B1, AhRR, TiPARP, IDO1, and AhR mRNA were all upregulated over

the course of infection (Fig. 4A). To determine if this response is conserved in other immune cell types, we quantified transcription of these downstream effectors in bone marrow-derived dendritic cells (BMDCs) (Fig. 4B). At both 12 and 22 hpi, CYP1B1, AhRR, TiPARP, IDO1, and AhR were all upregulated in BMDCs, suggesting that AhR activation occurs following MHV-A59 infection in multiple cell types.

To determine if our *in vitro* results could be recapitulated *in vivo*, we infected C57Bl/6 mice with MHV-A59 via intraperitoneal injection (Fig. 4C). At 3 and 5 days post infection (dpi), levels of CYP1B1, TiPARP, AhRR, and IDO1 mRNA increased in the livers of infected mice, suggesting that MHV elicited AhR activation. Furthermore, upregulation of these downstream genes paralleled viral replication at 3 and 5 dpi as assessed by measuring viral gRNA levels. In contrast to our results in BMDMs, IDO2 and TDO2 mRNA were detectable in liver samples and modestly increased on 3 dpi.

Consistent with the results obtained using infected livers, the level of AhR activation correlated with virus replication in BMDMs as downstream effector mRNA levels were less upregulated when cells were infected at lower MOIs (Fig. 5A). In addition, UV-inactivated virus infection was unable to induce expression of AhR downstream effectors, indicating that AhR activation during MHV infection is completely dependent on viral replication (Fig. 5B).

AhR antagonist and agonist treatment modulates expression of downstream effector genes during infection.

To examine whether AhR activation and not an alternative factor facilitated expression of these downstream effectors, we infected cells following chemical inhibition of AhR (Fig. 6A). We opted for treatment with CH-223191, a well-described chemical inhibitor that prevents ligand binding to AhR (Fig. 1) but does not inhibit other receptors such as the estrogen receptor (44, 45).

We first confirmed that CH-223191 inhibited chemical AhR activation by agonist TCDD in BMDMs without altering cell viability (Fig. 6B & C). During MHV-A59 infection, AhR inhibitor treatment resulted in dose-dependent attenuation of CYP1B1, AhRR, and IDO1. Surprisingly, TiPARP induction was not diminished at any concentration of inhibitor. Furthermore, CH-223191 treatment actually increased AhR mRNA levels slightly at 12 hpi but had no effect on gRNA levels, indicating that the CH-223191-mediated reduction in downstream effector expression was due to inhibition of AhR activation itself rather than decreased AhR expression or increased virus replication.

To complement these results and to determine if concurrent chemical activation during infection could further activate AhR, we treated BMDMs with TCDD and quantified induction of the same downstream effector genes that were attenuated by AhR inhibition (Fig. 7A). After confirming that TCDD that did not affect cell viability (Fig. 7B), we found that agonist treatment increased expression of CYP1B1 and AhRR compared to vehicle treatment in both mock- or MHV-infected BMDMs. TiPARP mRNA increased following TCDD treatment of uninfected cells and only marginally, if at all, after infection. IDO1 required infection for any expression and was potentiated by TCDD at 22 hpi. Finally, TCDD-treatment without or with infection resulted in small decreases in AhR expression in mock- and MHV-infected cells at 12 hpi but did not affect gRNA levels, again suggesting that agonist-induced changes in downstream effector expression was due primarily to AhR activation.

TiPARP is regulated by both IFN and the AhR during MHV infection.

TiPARP expression was induced by AhR agonist treatment (Fig. 7A) but did not change following inhibitor treatment during infection (Fig. 6A), suggesting MHV could also induce TiPARP expression by an AhR-independent mechanism. Because IFN-I treatment in BMDMs can

induce TiPARP expression (8), we next examined whether IFN-I upregulated TiPARP expression after inhibition of AhR activation. Using MHV-infected IFNAR$^{-/-}$ BMDMs treated with CH-223191, we observed a dose-dependent decrease in the expression of CYP1B1, AhRR, and IDO1 (Fig. 8), confirming that AhR activation did not require IFN signaling. In addition, AhR inhibitor treatment reduced TiPARP induction in IFNAR$^{-/-}$ BMDMs, indicating that AhR and IFN-I were compensatory in inducing TiPARP during infection. However, CH-223191-mediated reduction of TiPARP mRNA levels in IFNAR$^{-/-}$ BMDMs was less than that of CYP1B1, AhRR, or IDO1, suggesting that an additional, as yet unknown, factor modulated its expression. Finally, gRNA levels in IFNAR$^{-/-}$ BMDMs trended toward a modest reduction following AhR inhibition ($p=0.12$), possibly reflecting decreases in TiPARP expression. Taken together, our data show that MHV-induced AhR activation is responsible for upregulation of CYP1B1, AhRR, and IDO1 in IFN-replete and -deficient cells and of TiPARP in the absence of IFN-I signaling.

MHV infection activates AhR in an IDO1-independent manner.

While our results indicated that AhR activation during MHV-A59 infection modulates downstream IDO1 expression (Fig. 6 to Fig. 8), IDO1 can also act as an upstream regulator of AhR by catabolizing tryptophan to the AhR ligand kynurenine (Fig. 1) (13, 17). To determine if IDO1 has a role in AhR activation during MHV-A59 infection, we infected IDO1$^{-/-}$ BMDMs with MHV-A59 and quantified effector mRNA levels (Fig. 9B). Interestingly, levels of CYP1B1, AhRR, TiPARP, AhR, and gRNA were equivalent following infection in WT or IDO1$^{-/-}$ BMDMs. As expected, IDO1 mRNA was not detectable in deficient cells. To rule out compensatory effects of other enzymes known to produce kynurenine, we also assessed cells for IDO2 and TDO2 mRNA but could detect neither in WT or IDO1$^{-/-}$ BMDMs. Together, our results suggest that MHV-A59 infection of BMDMs elicits AhR activation through a pathway independent of IDO1.

MHV-induced AhR activation modulates cytokine production.

AhR activation can induce or modulate cytokine/chemokine production during the innate immune response (23). To determine whether AhR activation during CoV infection modulates cytokine expression, we infected CH-223191-treated BMDMs with MHV-A59 and quantified mRNA levels of IFNα4, β, and γ and of cytokines previously shown to be regulated by LPS-induced AhR activation in macrophages (TNFα ,IL-1β, and IL-10) (29, 30) (Fig. 10A). Inhibition of AhR had no impact on expression of IFNα4/β/γ mRNA. On the other hand, CH-223191 treatment resulted in a dose-dependent increase in the levels of TNFα mRNA and a concurrent decrease in the levels of IL-1β and IL-10 mRNA. Because AhR could be further activated during infection by chemical means (Fig. 7), we substantiated these findings by treating BMDMs with TCDD in the presence or absence of infection at low and high MOI (Fig. 10B). Consistent with our AhR inhibitor data, TNFα mRNA was decreased, and IL-1β and IL-10 mRNA were increased by concurrent chemical activation of AhR. In summary, these results indicate that AhR activation modulates multiple cytokine expression levels during MHV-A59 infection.

Discussion

Here, we showed that MHV infection activates AhR, resulting in upregulation of multiple downstream effector genes, including CYP1B1, AhRR, and IDO1, in infected BMDMs, BMDCs, and mouse livers (Fig. 4). We also demonstrated that another AhR downstream effector, TiPARP, has a pro-viral role on MHV replication as genomic RNA levels and virus titers were decreased following TiPARP knockdown (Fig. 3). TiPARP induction is a multifactorial manner, since IFN-I treatment induced TiPARP expression in BMDMs (8) but TiPARP expression was still observed in cell lines deficient in IFN expression and in IFNAR$^{-/-}$ BMDMs (Fig. 2). Our results showed that

AhR activation directly induces TiPARP expression as TCDD treatment enhanced TiPARP expression in uninfected and to a lesser extent in infected cells (Fig. 6). Further, TiPARP induction during infection was sensitive to chemical AhR inhibition in the absence but not the presence of IFN-I signaling in WT BMDMs (Fig. 6 and Fig. 8), consistent with redundant roles for AhR and IFN-I signaling in TiPARP expression during infection. Despite attenuation with inhibitor treatment, TiPARP expression in infected IFNAR$^{-/-}$ cells was still induced, indicating that other factors known to modulate TiPARP expression, such as estrogen receptor, glucocorticoid receptor, or TGFβ signaling pathways could also impact its expression during CoV infection (46-48).

In addition to decreased replication, TiPARP knockdown also resulted in increased IFNα4 and IFNβ mRNA expression (Fig. 3C). However, viral genomic RNA levels were reduced in TiPARP knockdown cells as early as 6 hpi, before IFN-I mRNA levels increased. Further study will be required to establish a causal relationship between the effects of TiPARP on IFN-I expression and replication. Our results align with a previous study showing that that TiPARP during IAV infection ADP-ribosylates TBK1, resulting in increased replication and reduced IFN-I levels (40). However, TiPARP has also been shown to bind to Sindbis virus RNA to trigger an antiviral host response. Therefore, it will be important to determine whether TiPARP facilitation of MHV replication is dependent on its ADP-ribosylating and/or its RNA-binding activities.

In contrast with TiPARP, upregulation of downstream effectors CYP1B1, AhRR, and IDO1 during infection is driven primarily by AhR activation. This is evidenced by the fact that expression of these effectors was enhanced by an AhR agonist and attenuated in a dose-dependent manner by an AhR-specific inhibitor (Fig. 6 and Fig. 7). While AhR activation has been studied in immune cells following treatment following agonist or immunostimulants treatment, its role in the context of virus infection is relatively understudied and only a few studies have details host

pathways affected by AhR activation. EBV encodes viral protein EBNA-3, which binds to ARNT and enhances transactivation of downstream effectors by AhR (41). AhR facilitates HCV infection by inducing expression of CYPs that aid in formation of lipid droplets required for virus production (38). As mentioned above, AhR functions in a pro-viral manner in IAV infection by inducing TiPARP (40). In contrast, AhR activation in HSV- or HIV-infected macrophages restricts replication by inhibiting expression of cyclins and cyclin-dependent kinases (39). Thus, AhR activation during viral infection has differing effects and modulates multiple cellular pathways, many of which remain uncharacterized.

Surprisingly, while AhR is thought to be activated primarily by kynurenine synthesized via IDO1 during inflammatory states and can drive positive feedback cycles in immune cells (17, 18), our results demonstrate that MHV infection activates AhR independent of IDO1 (Fig. 1 & 9). We detected gene expression of IDO2 and TDO2 in infected murine liver samples (Fig. 4C), consistent with the notion that TDO is largely constrained to the liver (14). While TDO or IDO2 could be driving AhR activation by producing kynurenine during *in vivo* infection, IDO2 and TDO mRNA were undetectable in in IDO1$^{-/-}$ BMDMs. This suggests that kynurenine is produced by a novel IDOI/IDO2/TDO-independent pathway in BMDMs or that these cells do not utilize kynurenine as the primary AhR ligand during CoV infection. AhR can be activated by several biochemical species, including metabolites of tryptophan or bilirubin or other metabolites of uncharacterized biosynthetic pathways (49-52). Other potential initiating pathways include prostaglandin synthesis, cAMP production, or general oxidative stress (20-22). Alternatively, a host or viral protein during infection could directly bind to AhR, enhancing its transactivation activity in a manner similar to that of EBV-encoded EBNA-3, though this may still require concomitant ligand binding (41). Nonetheless, the levels of the ligand or binding partner activating AhR in BMDMs

would likely scale with replication as downstream effector transcription correlated with virus load (Fig. 5). Additional investigation will be necessary to detail the exact mechanism of this IDO-independent AhR activation pathway. Furthermore, while IDO1 does not regulate AhR activation during MHV infection in BMDMs, it could still be modulating other cellular pathways as part of the host response. For instance, IDO1 has been shown to regulate immune cell function by mediating tryptophan starvation, resulting in activation of mTOR, a mediator of several metabolic and immune pathways (53, 54).

Finally, chemical activation or inhibition of AhR during infection resulted in changes in the mRNA levels of multiple cytokines (Fig. 10), suggesting that AhR functions to modulate the cytokine response to MHV infection. Specifically, AhR negatively regulated TNFα and positively regulated IL-1β and IL-10, cytokines which are also upregulated in the brains of MHV-infected mice (2). These changes were not due to alterations in viral replication, as viral load was unchanged by AhR activation or inhibition. The mechanism driving cytokine changes during MHV infection is likely complex but probably involves interaction of activated AhR with NF-κB (30, 33-35, 55) (Fig. 1). The effects of these cytokine expression changes will need to be investigated *in vivo* to determine their role in pathogenesis because their functions are protean because some of these cytokines are additionally post-transcriptionally regulated, and because activating ligands may differ in cultured BMDMs versus infected mice. Thus, it is difficult to conclude at present that AhR drives a strictly pro- or anti-inflammatory phenotype. Rather, AhR activation may serve to fine tune the innate immune response to MHV infection.

Methods

Mice. Pathogen-free C57BL/6 WT and IFNAR$^{-/-}$ mice were purchased from Jackson Laboratories, and IDO1$^{-/-}$ mice were obtained as a generous gift from Dr. Mark Santillan (University of Iowa, Iowa City, Iowa). IFN$\gamma^{-/-}$ mice were obtained from Jackson Laboratories. All mice were bred and maintained in the animal care facility at the University of Iowa as approved by the University of Iowa Institutional Animal Care and Use Committee (IACUC) following guidelines set forth by the Guide for the Care and Use of Laboratory Animals.

Cell cultures. Delayed brain tumor (DBT) cells, 17Cl-1 cells, and HeLa cells expressing the MHV receptor carcinoembryonic antigen-related cell adhesion molecule 1 (CEACAM1) (HeLa-MHVR), were grown in Dulbecco's Modified Eagle Medium (DMEM) supplemented with 10% fetal bovine serum (FBS), 100 U/ml penicillin, and 100 µg/ml streptomycin. Bone marrow cells obtained from WT, IFNAR$^{-/-}$, and IDO1$^{-/-}$ C57BL/6 mice were differentiated into macrophages (BMDMs) by incubating cells with 10% L929 cell supernatant and 10% FBS in Roswell Park Memorial Institute (RPMI) media for 7-8 days. BMDMs were washed and replaced with fresh media every day after the 4th day. Bone marrow cells obtained from WT C57BL/6 mice were differentiated into dendritic cells (BMDCs) by incubating cells with 50 µg/ml granulocyte/macrophage colony stimulating factor (GM-CSF) and 20 µg/ml IL-4. Extra media was added at day 3 to refresh the cells, media was fully changed on day 6, and cells were used for infections on day 7.

Virus infection. Mouse hepatitis virus (MHV) strain A59 (MHV-A59) (56) was propagated on 17Cl-1 cells in the same manner as described previously (8). BMDMs were infected with virus at indicated MOIs with a 45 min adsorption phase. At the indicated time points, cells were lysed with Trizol for RNA isolation, or cells were frozen with supernatants for titering on HeLa cells. To generate replication-deficient virus, MHV-A59 stocks were UV-inactivated using

a biosafety cabinet UV lamp for 30 min at room temperature. Inactivation was confirmed by plaque assay. For AhR agonist studies, media with 10 nM TCDD was added after mock adsorption or adsorption with MHV-A59. For chemical inhibitor studies, BMDMs were pretreated with 0.2, 1 or 5 μM CH-223191 (Sigma-Aldrich) vehicle (0.01% DMSO) for 2-6 h prior to infection or to treatment with 10 nM TCDD. After TCDD treatment or infection, media containing inhibitors was added back to cells. For mouse infections, 5-8-week-old mice were anesthetized with ketamine/xylazine and inoculated intraperitoneally with 10^4 PFU of MHV-A59 in 300 μL DMEM or with mock (DMEM only). Mice were sacrificed at 3 and 5 dpi, and livers were harvested and stored in Trizol (Thermo Fisher Scientific).

siRNA transfection. BMDMs were transfected with 50 pmol/ml of siRNA with Viromer BLUE (Lipocalyx) following the manufacturer's protocol. Media was replaced 4 h after transfection, and cells were infected 28 h post transfection. The sequences of negative (non-specific) control DsiRNA were sense: CGUUAAUCGCGUAUAAUACGCGUAT and antisense: AUACGCGUAUUAUACGCGAUUAACGAC. The sequences of DsiRNA oligonucleotides directed toward TiPARP (Integrated DNA Technologies (IDT)) were sense: GAAGAUAAAAGUUAUCGAAUCAUTT and antisense: AAAUGAUUCGAUAACUUUUAUCUUCUG.

Real-time quantitative PCR (RT-qPCR) analysis. RNA was purified using Trizol (Thermo Fisher Scientific) by Direct-Zol columns (Zymo Research) or by phase separation as instructed by the manufacturer. cDNA was synthesized using MMLV-reverse transcriptase (Thermo Fisher Scientific) and quantified with a real-time thermocycler using PowerUp SYBR Green Master Mix (Thermo Fisher Scientific). RT-qPCR primers are listed in Table 1. Primers spanned exon-exon junctions when possible to avoid quantification of any residual genomic DNA.

A control without reverse transcriptase was also analyzed to confirm the absence of any contaminating DNA. Target genes were normalized to housekeeping gene hypoxanthine-guanine phosphoribosyltransferase (HPRT) by the following equation: $\Delta C_T = C_T$ (gene of interest) - C_T (HPRT). All results are shown as a ratio to HPRT calculated as $-2^{\Delta CT}$.

Cell viability assay. Viability/metabolism of BMDMs treated with 10 nM TCDD or 5 μM CH-223191 for 12 or 24 h was assessed using a Vybrant MTT Cell Proliferation Assay (Thermo Fisher Scientific) as per manufacturer's instructions. Cell viability was measured by absorbance at 540 nm (A_{540}).

Statistics. An unpaired two-tailed Student's t-test was used to determine statistically significant differences in means between group. All graphs are expressed as mean ± SEM. The n value represents the number of biologic replicates for each figure. Multiple trials were combined into a single figure when expression values or titers were comparable. Significant p values are annotated as *$p \leq 0.05$, **$p \leq 0.01$, ***$p \leq 0.001$. If the p value was less than 0.15 but greater than 0.05, the numerical value was listed above the graph bars and was considered trending towards significance.

Acknowledgements

We thank members of the Perlman laboratory and Drs. Wendy Maury and Aloysius Klingelhutz for valuable discussion; Dr. Mark Santillan for mice; Alan Sariol for assistance with mouse experiments; and Dr. Aloysius Klingelhutz for critical reading of this manuscript.

This study was supported in part by grants from the NIH (ROI NS36592 (S.P.), CoBRE P20 GM113117-02 (A.R.F.), K22 AI134993-01(A.R.F.)), and the University of Kansas (A.R.F.).

References

1. **Fehr AR, Perlman S.** 2015. Coronaviruses: an overview of their replication and pathogenesis. Methods Mol Biol **1282:**1-23.
2. **Bergmann CC, Lane TE, Stohlman SA.** 2006. Coronavirus infection of the central nervous system: host-virus stand-off. Nat Rev Microbiol **4:**121-132.
3. **Roth-Cross JK, Bender SJ, Weiss SR.** 2008. Murine coronavirus mouse hepatitis virus is recognized by MDA5 and induces type I interferon in brain macrophages/microglia. J Virol **82:**9829-9838.
4. **Ireland DD, Stohlman SA, Hinton DR, Atkinson R, Bergmann CC.** 2008. Type I interferons are essential in controlling neurotropic coronavirus infection irrespective of functional CD8 T cells. J Virol **82:**300-310.
5. **Zhou H, Perlman S.** 2006. Preferential infection of mature dendritic cells by mouse hepatitis virus strain JHM. J Virol **80:**2506-2514.
6. **Zhou H, Perlman S.** 2007. Mouse hepatitis virus does not induce Beta interferon synthesis and does not inhibit its induction by double-stranded RNA. J Virol **81:**568-574.
7. **Versteeg GA, Bredenbeek PJ, van den Worm SH, Spaan WJ.** 2007. Group 2 coronaviruses prevent immediate early interferon induction by protection of viral RNA from host cell recognition. Virology **361:**18-26.
8. **Grunewald ME, Chen Y, Kuny C, Maejima T, Lease R, Ferraris D, Aikawa M, Sullivan CS, Perlman S, Fehr AR.** 2019. The coronavirus macrodomain is required to prevent PARP-mediated inhibition of virus replication and enhancement of IFN expression. PLoS Pathog **15:**e1007756.
9. **Fehr AR, Channappanavar R, Jankevicius G, Fett C, Zhao J, Athmer J, Meyerholz DK, Ahel I, Perlman S.** 2016. The Conserved Coronavirus Macrodomain Promotes Virulence and Suppresses the Innate Immune Response during Severe Acute Respiratory Syndrome Coronavirus Infection. MBio. **7**(6)**:**doi:10.1128/mBio.01721-16.
10. **Gutierrez-Vazquez C, Quintana FJ.** 2018. Regulation of the Immune Response by the Aryl Hydrocarbon Receptor. Immunity **48:**19-33.
11. **Mimura J, Ema M, Sogawa K, Fujii-Kuriyama Y.** 1999. Identification of a novel mechanism of regulation of Ah (dioxin) receptor function. Genes Dev **13:**20-25.
12. **Ahmed S, Bott D, Gomez A, Tamblyn L, Rasheed A, Cho T, MacPherson L, Sugamori KS, Yang Y, Grant DM, Cummins CL, Matthews J.** 2015. Loss of the Mono-ADP-ribosyltransferase, Tiparp, Increases Sensitivity to Dioxin-induced Steatohepatitis and Lethality. J Biol Chem **290:**16824-16840.
13. **Opitz CA, Litzenburger UM, Sahm F, Ott M, Tritschler I, Trump S, Schumacher T, Jestaedt L, Schrenk D, Weller M, Jugold M, Guillemin GJ, Miller CL, Lutz C, Radlwimmer B, Lehmann I, von Deimling A, Wick W, Platten M.** 2011. An endogenous tumour-promoting ligand of the human aryl hydrocarbon receptor. Nature **478:**197-203.
14. **Mellor AL, Munn DH.** 2004. IDO expression by dendritic cells: tolerance and tryptophan catabolism. Nat Rev Immunol **4:**762-774.
15. **Murakami Y, Hoshi M, Imamura Y, Arioka Y, Yamamoto Y, Saito K.** 2013. Remarkable role of indoleamine 2,3-dioxygenase and tryptophan metabolites in infectious diseases: potential role in macrophage-mediated inflammatory diseases. Mediators Inflamm **2013:**391984.

16. **Pallotta MT, Fallarino F, Matino D, Macchiarulo A, Orabona C.** 2014. AhR-Mediated, Non-Genomic Modulation of IDO1 Function. Front Immunol **5:**497.
17. **Litzenburger UM, Opitz CA, Sahm F, Rauschenbach KJ, Trump S, Winter M, Ott M, Ochs K, Lutz C, Liu X, Anastasov N, Lehmann I, Hofer T, von Deimling A, Wick W, Platten M.** 2014. Constitutive IDO expression in human cancer is sustained by an autocrine signaling loop involving IL-6, STAT3 and the AHR. Oncotarget **5:**1038-1051.
18. **Li Q, Harden JL, Anderson CD, Egilmez NK.** 2016. Tolerogenic Phenotype of IFN-gamma-Induced IDO+ Dendritic Cells Is Maintained via an Autocrine IDO-Kynurenine/AhR-IDO Loop. J Immunol **197:**962-970.
19. **Wincent E, Amini N, Luecke S, Glatt H, Bergman J, Crescenzi C, Rannug A, Rannug U.** 2009. The suggested physiologic aryl hydrocarbon receptor activator and cytochrome P4501 substrate 6-formylindolo[3,2-b]carbazole is present in humans. J Biol Chem **284:**2690-2696.
20. **Oesch-Bartlomowicz B, Huelster A, Wiss O, Antoniou-Lipfert P, Dietrich C, Arand M, Weiss C, Bockamp E, Oesch F.** 2005. Aryl hydrocarbon receptor activation by cAMP vs. dioxin: divergent signaling pathways. Proc Natl Acad Sci U S A **102:**9218-9223.
21. **Seidel SD, Winters GM, Rogers WJ, Ziccardi MH, Li V, Keser B, Denison MS.** 2001. Activation of the Ah receptor signaling pathway by prostaglandins. J Biochem Mol Toxicol **15:**187-196.
22. **Wincent E, Bengtsson J, Mohammadi Bardbori A, Alsberg T, Luecke S, Rannug U, Rannug A.** 2012. Inhibition of cytochrome P4501-dependent clearance of the endogenous agonist FICZ as a mechanism for activation of the aryl hydrocarbon receptor. Proc Natl Acad Sci U S A **109:**4479-4484.
23. **Rothhammer V, Quintana FJ.** 2019. The aryl hydrocarbon receptor: an environmental sensor integrating immune responses in health and disease. Nat Rev Immunol **19:**184-197.
24. **Gandhi R, Kumar D, Burns EJ, Nadeau M, Dake B, Laroni A, Kozoriz D, Weiner HL, Quintana FJ.** 2010. Activation of the aryl hydrocarbon receptor induces human type 1 regulatory T cell-like and Foxp3(+) regulatory T cells. Nat Immunol **11:**846-853.
25. **Quintana FJ, Basso AS, Iglesias AH, Korn T, Farez MF, Bettelli E, Caccamo M, Oukka M, Weiner HL.** 2008. Control of T(reg) and T(H)17 cell differentiation by the aryl hydrocarbon receptor. Nature **453:**65-71.
26. **Apetoh L, Quintana FJ, Pot C, Joller N, Xiao S, Kumar D, Burns EJ, Sherr DH, Weiner HL, Kuchroo VK.** 2010. The aryl hydrocarbon receptor interacts with c-Maf to promote the differentiation of type 1 regulatory T cells induced by IL-27. Nat Immunol **11:**854-861.
27. **Quintana FJ, Murugaiyan G, Farez MF, Mitsdoerffer M, Tukpah AM, Burns EJ, Weiner HL.** 2010. An endogenous aryl hydrocarbon receptor ligand acts on dendritic cells and T cells to suppress experimental autoimmune encephalomyelitis. Proc Natl Acad Sci U S A **107:**20768-20773.
28. **Bankoti J, Rase B, Simones T, Shepherd DM.** 2010. Functional and phenotypic effects of AhR activation in inflammatory dendritic cells. Toxicol Appl Pharmacol **246:**18-28.
29. **Sekine H, Mimura J, Oshima M, Okawa H, Kanno J, Igarashi K, Gonzalez FJ, Ikuta T, Kawajiri K, Fujii-Kuriyama Y.** 2009. Hypersensitivity of aryl hydrocarbon receptor-deficient mice to lipopolysaccharide-induced septic shock. Mol Cell Biol **29:**6391-6400.

30. **Kimura A, Naka T, Nakahama T, Chinen I, Masuda K, Nohara K, Fujii-Kuriyama Y, Kishimoto T.** 2009. Aryl hydrocarbon receptor in combination with Stat1 regulates LPS-induced inflammatory responses. J Exp Med **206:**2027-2035.
31. **Masuda K, Kimura A, Hanieh H, Nguyen NT, Nakahama T, Chinen I, Otoyo Y, Murotani T, Yamatodani A, Kishimoto T.** 2011. Aryl hydrocarbon receptor negatively regulates LPS-induced IL-6 production through suppression of histamine production in macrophages. Int Immunol **23:**637-645.
32. **Veldhoen M, Hirota K, Westendorf AM, Buer J, Dumoutier L, Renauld JC, Stockinger B.** 2008. The aryl hydrocarbon receptor links TH17-cell-mediated autoimmunity to environmental toxins. Nature **453:**106-109.
33. **Vogel CF, Matsumura F.** 2009. A new cross-talk between the aryl hydrocarbon receptor and RelB, a member of the NF-kappaB family. Biochem Pharmacol **77:**734-745.
34. **Vogel CF, Khan EM, Leung PS, Gershwin ME, Chang WL, Wu D, Haarmann-Stemmann T, Hoffmann A, Denison MS.** 2014. Cross-talk between aryl hydrocarbon receptor and the inflammatory response: a role for nuclear factor-kappaB. J Biol Chem **289:**1866-1875.
35. **Salisbury RL, Sulentic CE.** 2015. The AhR and NF-kappaB/Rel Proteins Mediate the Inhibitory Effect of 2,3,7,8-Tetrachlorodibenzo-p-Dioxin on the 3' Immunoglobulin Heavy Chain Regulatory Region. Toxicol Sci **148:**443-459.
36. **Salazar F, Awuah D, Negm OH, Shakib F, Ghaemmaghami AM.** 2017. The role of indoleamine 2,3-dioxygenase-aryl hydrocarbon receptor pathway in the TLR4-induced tolerogenic phenotype in human DCs. Sci Rep **7:**43337.
37. **Bessede A, Gargaro M, Pallotta MT, Matino D, Servillo G, Brunacci C, Bicciato S, Mazza EM, Macchiarulo A, Vacca C, Iannitti R, Tissi L, Volpi C, Belladonna ML, Orabona C, Bianchi R, Lanz TV, Platten M, Della Fazia MA, Piobbico D, Zelante T, Funakoshi H, Nakamura T, Gilot D, Denison MS, Guillemin GJ, DuHadaway JB, Prendergast GC, Metz R, Geffard M, Boon L, Pirro M, Iorio A, Veyret B, Romani L, Grohmann U, Fallarino F, Puccetti P.** 2014. Aryl hydrocarbon receptor control of a disease tolerance defence pathway. Nature **511:**184-190.
38. **Ohashi H, Nishioka K, Nakajima S, Kim S, Suzuki R, Aizaki H, Fukasawa M, Kamisuki S, Sugawara F, Ohtani N, Muramatsu M, Wakita T, Watashi K.** 2018. The aryl hydrocarbon receptor-cytochrome P450 1A1 pathway controls lipid accumulation and enhances the permissiveness for hepatitis C virus assembly. J Biol Chem **293:**19559-19571.
39. **Kueck T, Cassella E, Holler J, Kim B, Bieniasz PD.** 2018. The aryl hydrocarbon receptor and interferon gamma generate antiviral states via transcriptional repression. Elife. **7**(doi:10.7554/eLife.38867.
40. **Yamada T, Horimoto H, Kameyama T, Hayakawa S, Yamato H, Dazai M, Takada A, Kida H, Bott D, Zhou AC, Hutin D, Watts TH, Asaka M, Matthews J, Takaoka A.** 2016. Constitutive aryl hydrocarbon receptor signaling constrains type I interferon-mediated antiviral innate defense. Nat Immunol **17:**687-694.
41. **Kashuba EV, Gradin K, Isaguliants M, Szekely L, Poellinger L, Klein G, Kazlauskas A.** 2006. Regulation of transactivation function of the aryl hydrocarbon receptor by the Epstein-Barr virus-encoded EBNA-3 protein. J Biol Chem **281:**1215-1223.
42. **Navas S, Weiss SR.** 2003. Murine coronavirus-induced hepatitis: JHM genetic background eliminates A59 spike-determined hepatotropism. J Virol **77:**4972-4978.

43. **Ma Q, Baldwin KT, Renzelli AJ, McDaniel A, Dong L.** 2001. TCDD-inducible poly(ADP-ribose) polymerase: a novel response to 2,3,7,8-tetrachlorodibenzo-p-dioxin. Biochem Biophys Res Commun **289:**499-506.
44. **Kim SH, Henry EC, Kim DK, Kim YH, Shin KJ, Han MS, Lee TG, Kang JK, Gasiewicz TA, Ryu SH, Suh PG.** 2006. Novel compound 2-methyl-2H-pyrazole-3-carboxylic acid (2-methyl-4-o-tolylazo-phenyl)-amide (CH-223191) prevents 2,3,7,8-TCDD-induced toxicity by antagonizing the aryl hydrocarbon receptor. Mol Pharmacol **69:**1871-1878.
45. **Zhao B, Degroot DE, Hayashi A, He G, Denison MS.** 2010. CH223191 is a ligand-selective antagonist of the Ah (Dioxin) receptor. Toxicol Sci **117:**393-403.
46. **Reddy TE, Pauli F, Sprouse RO, Neff NF, Newberry KM, Garabedian MJ, Myers RM.** 2009. Genomic determination of the glucocorticoid response reveals unexpected mechanisms of gene regulation. Genome Res **19:**2163-2171.
47. **Chen WV, Delrow J, Corrin PD, Frazier JP, Soriano P.** 2004. Identification and validation of PDGF transcriptional targets by microarray-coupled gene-trap mutagenesis. Nat Genet **36:**304-312.
48. **Kininis M, Chen BS, Diehl AG, Isaacs GD, Zhang T, Siepel AC, Clark AG, Kraus WL.** 2007. Genomic analyses of transcription factor binding, histone acetylation, and gene expression reveal mechanistically distinct classes of estrogen-regulated promoters. Mol Cell Biol **27:**5090-5104.
49. **Heath-Pagliuso S, Rogers WJ, Tullis K, Seidel SD, Cenijn PH, Brouwer A, Denison MS.** 1998. Activation of the Ah receptor by tryptophan and tryptophan metabolites. Biochemistry **37:**11508-11515.
50. **Bittinger MA, Nguyen LP, Bradfield CA.** 2003. Aspartate aminotransferase generates proagonists of the aryl hydrocarbon receptor. Mol Pharmacol **64:**550-556.
51. **Song J, Clagett-Dame M, Peterson RE, Hahn ME, Westler WM, Sicinski RR, DeLuca HF.** 2002. A ligand for the aryl hydrocarbon receptor isolated from lung. Proc Natl Acad Sci U S A **99:**14694-14699.
52. **Phelan D, Winter GM, Rogers WJ, Lam JC, Denison MS.** 1998. Activation of the Ah receptor signal transduction pathway by bilirubin and biliverdin. Arch Biochem Biophys **357:**155-163.
53. **Metz R, Rust S, Duhadaway JB, Mautino MR, Munn DH, Vahanian NN, Link CJ, Prendergast GC.** 2012. IDO inhibits a tryptophan sufficiency signal that stimulates mTOR: A novel IDO effector pathway targeted by D-1-methyl-tryptophan. Oncoimmunology **1:**1460-1468.
54. **Orabona C, Grohmann U.** 2011. Indoleamine 2,3-dioxygenase and regulatory function: tryptophan starvation and beyond. Methods Mol Biol **677:**269-280.
55. **Vogel CF, Sciullo E, Matsumura F.** 2007. Involvement of RelB in aryl hydrocarbon receptor-mediated induction of chemokines. Biochem Biophys Res Commun **363:**722-726.
56. **Yount B, Denison MR, Weiss SR, Baric RS.** 2002. Systematic assembly of a full-length infectious cDNA of mouse hepatitis virus strain A59. J Virol **76:**11065-11078.

560 **Figure legends**

561 **Figure 1. Schematic diagram of AhR activation in MHV-infected cells.** Ligands that can bind
562 to AhR can be exogenous (pentagon), such as toxins like 2,3,7,8-tetrachlorodibenzodioxin
563 (TCDD), or endogenous metabolic products (parallelogram), such as kynurenine derived by IDO1-
564 catalyzed tryptophan degradation. CoV infection produces an unknown AhR-activating ligand
565 independent of IDO1 (triangle). AhR in the cytosol is activated upon ligand binding and
566 translocates to the nucleus to bind to genomic DNA. The specific genes targeted and induced by
567 AhR are influenced by AhR binding partners including ARNT and NF-κB. Modulated genes
568 include AhR downstream effectors such as cytochrome P450 enzymes (CYPs), AhR repressor
569 (AhRR), and TiPARP or immune proteins such as cytokines. AhR activation/ligand binding can
570 be inhibited chemically by treatment with CH-223191.

571

572 **Figure 2. MHV-A59 infection upregulates TiPARP in cells lines and primary cells in the**
573 **absence of IFN-I signaling.** (A-B) DBT (A) or 17Cl-1 (B) cell lines were infected with MHV-
574 A59 at an MOI of 0.1 PFU/cell. Cells were collected at 18 hpi, and RNA was quantified qRT-PCR
575 with primers for the indicated PARPs. (C-D) WT (C) or WT and IFNAR$^{-/-}$ (D) BMDMs were mock
576 infected or infected with MHV-A59 at an MOI of 5 (C) or 0.1 (D) PFU/cell. Cells were collected
577 at 18 hpi, and mRNA was analyzed for quantified by qRT-PCR with primers for the indicated
578 PARPs. The data in (A-D) show one experiment representative of three independent experiments;
579 n=3. ns = not significant; nd = not detectable.

580

581 **Figure 3. MHV replication is diminished following TiPARP knockdown in BMDMs.** WT
582 BMDMs were transfected with siRNA targeting TiPARP and were then infected at 30 h post

583 transfection with MHV-A59 at MOI of 0.1 (A-B) or 5 PFU/cell (C-D). RNA was quantified by
584 qRT-PCR with primers specific for viral genomic RNA (gRNA) or for indicated transcripts (A, C),
585 or virus titers were determined by freezing-thawing cells followed by plaque assay on HeLa cells
586 expressing the MHV receptor (B, D). RNA and cell collections occurred at 12 hpi for MOI of 0.1
587 PFU/cell (A-B) or at 6, 12, 18, and 22 hpi for MOI of 5 PFU/cell (C-D). The data in (A,C) show
588 one experiment representative of at least two independent experiments; n=3. The data in (B,D)
589 show combined results of 2 experiments; n=6. ns = not significant.
590
591 **Figure 4. MHV infection results in upregulation of AhR downstream effector genes in**
592 **BMDMs, BMDCs, and *in vivo*.** (A) BMDMs were infected with MHV-A59 at an MOI of 5
593 PFU/cell and collected at the indicated time points. mRNA levels of downstream effector genes,
594 AhR, or IDO1 were then quantified by qRT-PCR. (B) BMDCs were infected with MHV-A59 at an
595 MOI of 5 PFU/cell and collected at 12 or 22 hpi. mRNA levels of indicated genes were quantified
596 by qRT-PCR. The data in (A,B) show one experiment representative of two independent
597 experiments; n=3. (C) C57BL/6 mice were intraperitoneally infected with 10^4 PFU of MHV-A59,
598 and perfused livers were harvested at 3 and 5 dpi. RNA was isolated, and mRNA levels of
599 downstream effectors, AhR, or kynurenine-producing enzymes were quantified by qRT-PCR. The
600 data in (C) show one experiment representative of three independent experiments; n=4. nd = not
601 detectable.
602
603 **Figure 5. Virus replication is correlated with and required for expression of AhR downstream**
604 **effectors during infection.** (A) BMDMs were infected with MHV-A59 at the indicated MOIs.
605 Cells were then collected at 12 hpi, and downstream effector, AhR, or IDO1 mRNA levels were

606 quantified by qRT-PCR. (B) BMDMs were infected with untreated or UV-inactivated virus at an
607 MOI of 5 PFU/cell. Expression of indicated genes was quantified by qRT-PCR. The data in (A,B)
608 show one experiment representative of two independent experiments; n=3. nd = not detectable.
609
610 **Figure 6. Chemical inhibition of AhR during MHV infection results in attenuated expression**
611 **of downstream genes.** (A) WT BMDMs were pretreated with vehicle (0.01% DMSO) or 0.2, 1,
612 or 5 μM CH-223191 and infected with MHV-A59 at an MOI of 5 PFU/cell. RNA was collected at
613 12 or 22 hpi and quantified for mRNA levels of downstream effectors, AhR, IDO1, or gRNA by
614 qRT-PCR. The data in (A) show one experiment representative of three independent experiments;
615 n=3. (B) Viability of BMDM cells treated with vehicle or 5 μM CH-223191 was quantified by
616 MTT assay at 12 and 24 hours post treatment. The data in (B) show one experiment representative
617 of two independent experiments; n=4. (C) CH-223191 inhibitor efficacy was determined by
618 preincubating uninfected BMDMs with vehicle (0.01% DMSO) or 5 μM CH-223191 followed by
619 addition of vehicle or 10 nM TCDD. At 12 h, RNA was harvested, and mRNA levels of
620 downstream effectors were determined by qRT-PCR. The data in (C) show one experiment
621 representative of two independent experiments; n=3. ns = not significant; nd = not detectable.
622
623 **Figure 7. Chemical activation of AhR in the absence and presence of infection enhances**
624 **expression of downstream genes.** (A) WT BMDMs were treated with vehicle (0.01% DMSO) or
625 10 nM of TCDD and concurrently mock-infected or infected with MHV-A59 at an MOI of 0.1 or
626 5 PFU/cell. RNA was collected at 12 or 22 hpi and quantified for mRNA levels of downstream
627 effectors, AhR, IDO1, or gRNA by qRT-PCR. The data in (A) show one experiment representative
628 of two independent experiments; n=3. (B) Viability of BMDM cells treated with vehicle or 10 nM

TCDD was quantified by MTT assay at 12 and 24 hours post treatment. The data in (B) show one experiment representative of two independent experiments; n=4. ns = not significant; nd = not detectable.

Figure 8. Infection upregulates TiPARP through redundant mechanisms requiring AhR activation or IFN-I signaling. BMDMs from IFNAR$^{-/-}$ mice were pretreated with vehicle (0.01% DMSO) or 0.2, 1, or 5 μM CH-223191 (223) and infected with MHV-A59 at an MOI of 5 PFU/cell. RNA was collected at 12 or 22 hpi and quantified for mRNA levels of downstream effectors, AhR, IDO1, or gRNA by qRT-PCR. The data show one experiment representative of two independent experiments; n=3. ns = not significant; nd = not detectable.

Figure 9. IDO1 expression is dispensable for MHV-mediated AhR activation. BMDMs from WT or IDO1$^{-/-}$ mice were infected with MHV-A59 at an MOI of 5 PFU/cell. RNA was collected at 12 or 22 hpi, and expression of indicated genes was quantified by qRT-PCR. The data show one experiment representative of two independent experiments; n=3. ns = not significant; nd = not detectable.

Figure 10. Inhibition or enhancement of AhR activation during MHV infection modulates cytokine expression. (A) WT BMDMs were pretreated with vehicle (0.01% DMSO) or 0.2, 1 or 5 μM CH-223191 and then infected at an MOI of 5 PFU/cell. RNA was collected and quantified at 22 hpi for mRNA levels of indicated cytokines by qRT-PCR. The data in (A) show one experiment representative of three independent experiments; n=3. (B) WT BMDMs were treated with vehicle (0.01% DMSO) or 10 nM TCDD and concurrently infected with MHV-A59 at an

652 MOI of 0.1 or 5 PFU/cell. RNA was collected and quantified at 22 hpi for mRNA levels of
653 indicated cytokines by qRT-PCR. The data in (B) show one experiment representative of two
654 independent experiments; n=3. ns = not significant; nd = not detectable.

655 **Table 1. Quantitative real-time qPCR primers.**

Gene	Forward 5'→3'	Reverse 5'→3'
HPRT	GCGTCGTGATTAGCGATGATG	CTCGAGCAAGTCTTTCAGTCC
PARP1	CAGGAGAGTCAGCGATCTTGG	ACCCATTCCTTTCGGCTAGG
PARP2	TGGAAGGCGAGTGCTAAATG	GGGCTTTGCCCTTTAACAGC
PARP3	TGCGGCATGTTTGGAAAGTG	GTGCATGGTGGTAACATAGCC
PARP4	AGTGCTACAGCCCGTTTCC	CACAGCTTTCAGTTGTGGGC
PARP5a	CCCTGAGGCCTTACCTACCT	TCAAGACCCGCAACTTCTCC
PARP5b	TGATGGCAGAAAGTCAACTCCA	GCCACAGGTCCATTGCATTC
PARP6	GTACCTTGATGGACCAGAGCC	GCCAGCTCGGAACTTCTTGA
PARP7	ATTTACAGACACTTGGTGGGG	GGCACTTGGATGAAGTCCTGA
PARP8	CACTTCCGAAACCACTTCGC	TAGGATACACTTTTGGGGCCG
PARP9	GCATTTGCTAAAGAGCACAAGGA	AAAGCACCACTATTACCGCTGA
PARP10	CGAAACGGCACACTCTACGG	GAGACCCTCAAAGGAGGTGC
PARP11	GGCTGTCTTTGGAAAAGGAACC	GCACTCGAGCAAGAAACATGG
PARP12	AGACCGGGAAGAACTGTAGGA	TTTGGAAGGAGCAAGAGCCG
PARP13	AGTAGTCCCACTGGTTTTGGC	TGCAACTCTGTGGCTTGTGG
PARP14	TGCTGAAGCTGTCAAGACTACA	ACAATGGCATGGGTCGTAGC
PARP16	CTTTGACCCGGCCAACTCC	AAACAGAGAAGTCTTGTTCAGGTG
gRNA	AGGGAGTTTGACCTTGTTCAG	ATAATGCACCTGTCATCCTCG
AhR	CCACTGACGGATGAAGAAGGA	ATCTCGTACAACACAGCCTCTC
CYP1A1	CAGGACATTTGAGAAGGGCCAC	GCTTCCTGTCCTGACAATGC
CYP1A2	TGGAGCTGGCTTTGACACAGT	GCCATGTCACAAGTAGCAAAATG
CYP1B1	GGCTTCATTAACAAGGCGCT	CACTGATGAGCGAGGATGGA
AhRR	GTTGGATCCTGTAGGGAGCA	AGTCCAGAGGCTCACGCTTA
IDO1	AGGATGCGTGACTTTGTGGA	TCCCAGACCCCCTCATACAG
IDO2	CTCAGACTTCCTCACTTAATCG	GCTGCTCACGGTAACTCT
TDO2	GTGAACGACGACTGTCATACCG	GCTGGAAAGGGACCTGGAAT
IFNα4	TCCATCAGCAGCTCAATGAC	AGGAAGAGAGGGCTCTCCAG
IFNβ	TCAGAATGAGTGGTGGTTGC	GACCTTTCAAATGCAGTAGATTCA
IFNγ	CGGCACAGTCATTGAAAGCCTA	GTTGCTGATGGCCTGATTGTC
TNFα	TCAGCCGATTTGCTATCTCA	CGGACTCCGCAAAGTCTAAG
IL-1β	ACTGTTTCTAATGCCTTCCC	ATGGTTTCTTGTGACCCTGA
IL-10	ATTTGAATTCCCTGGGTGAGAAG	CACAGGGGAGAAATCGATGACA

656

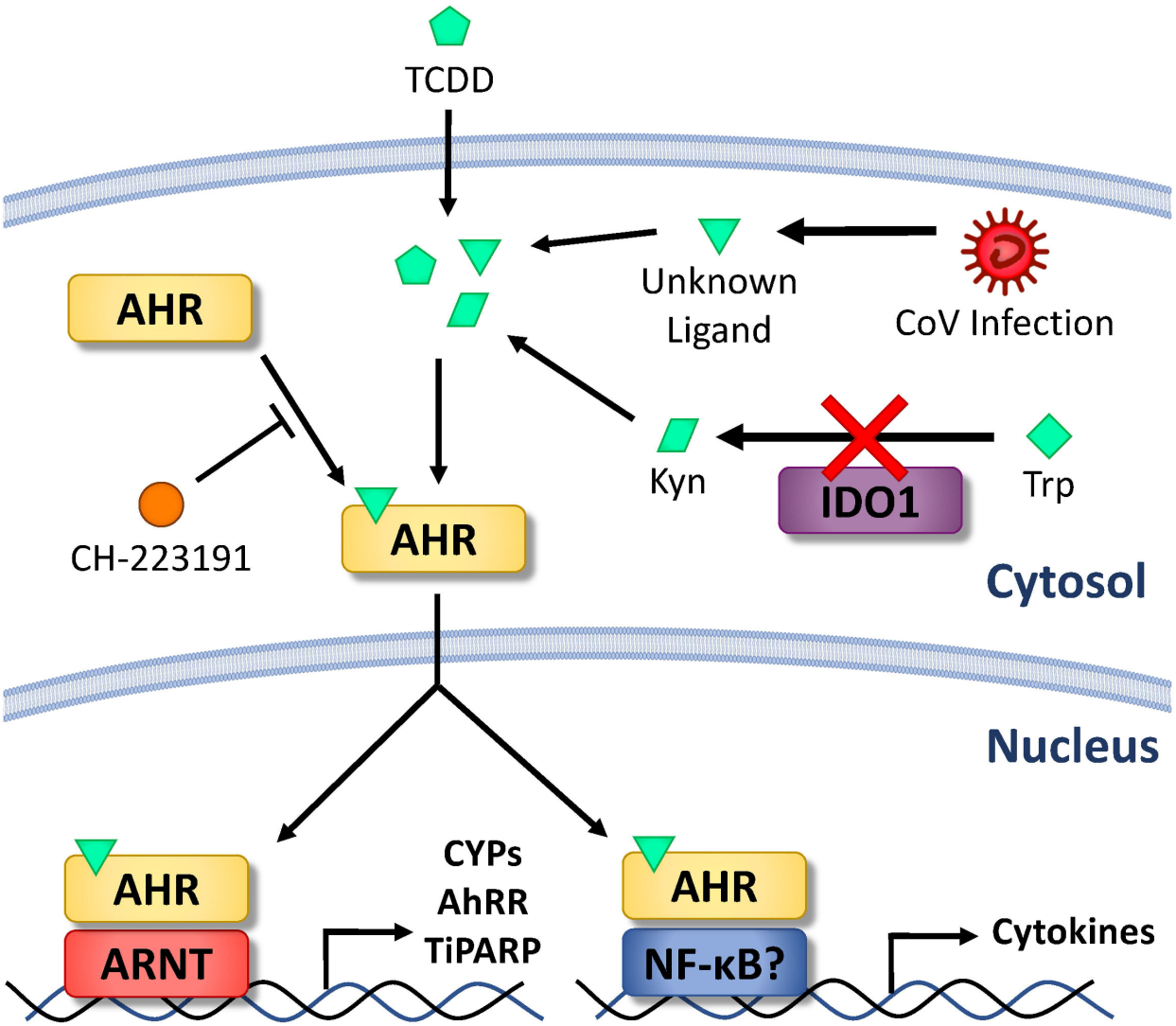

Journal of Virology

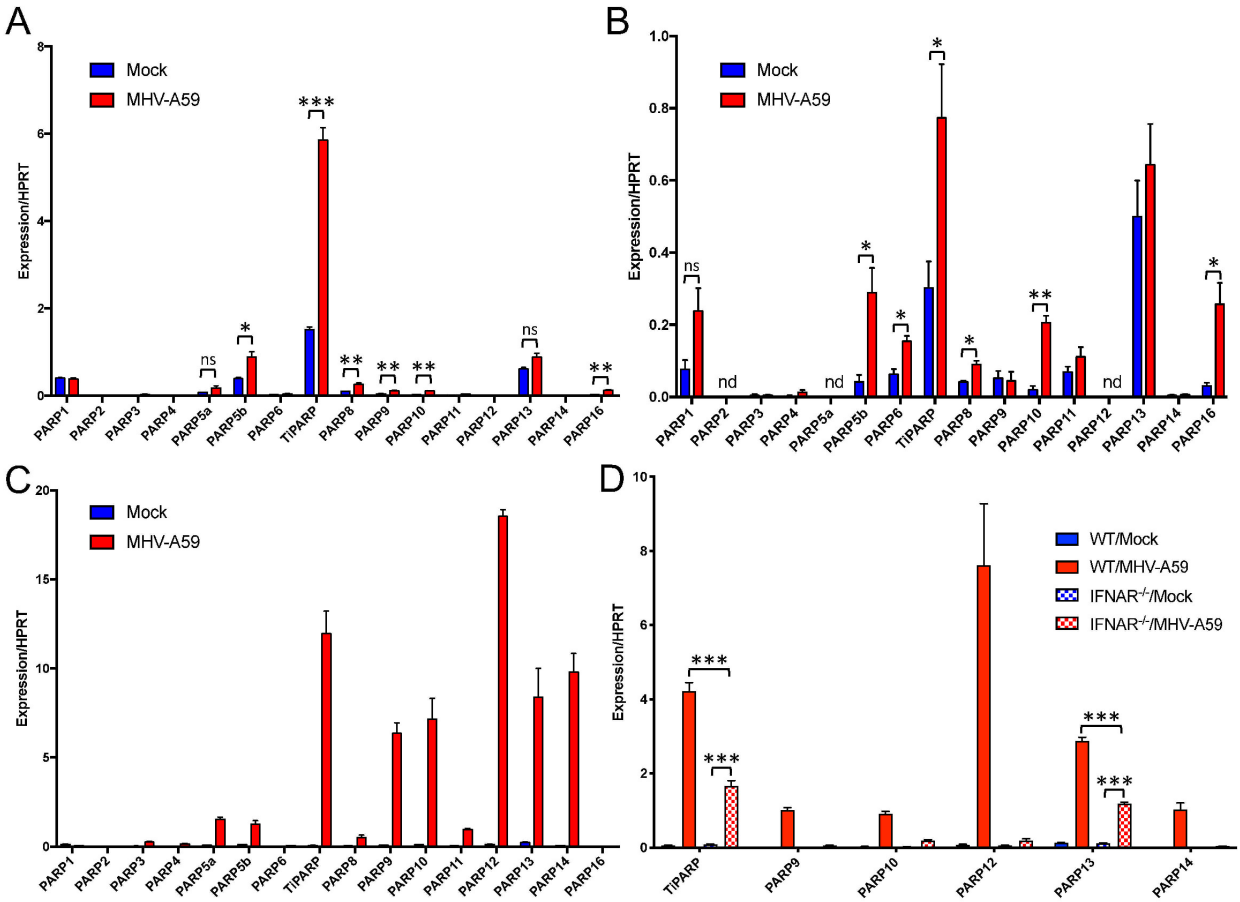

Journal of Virology

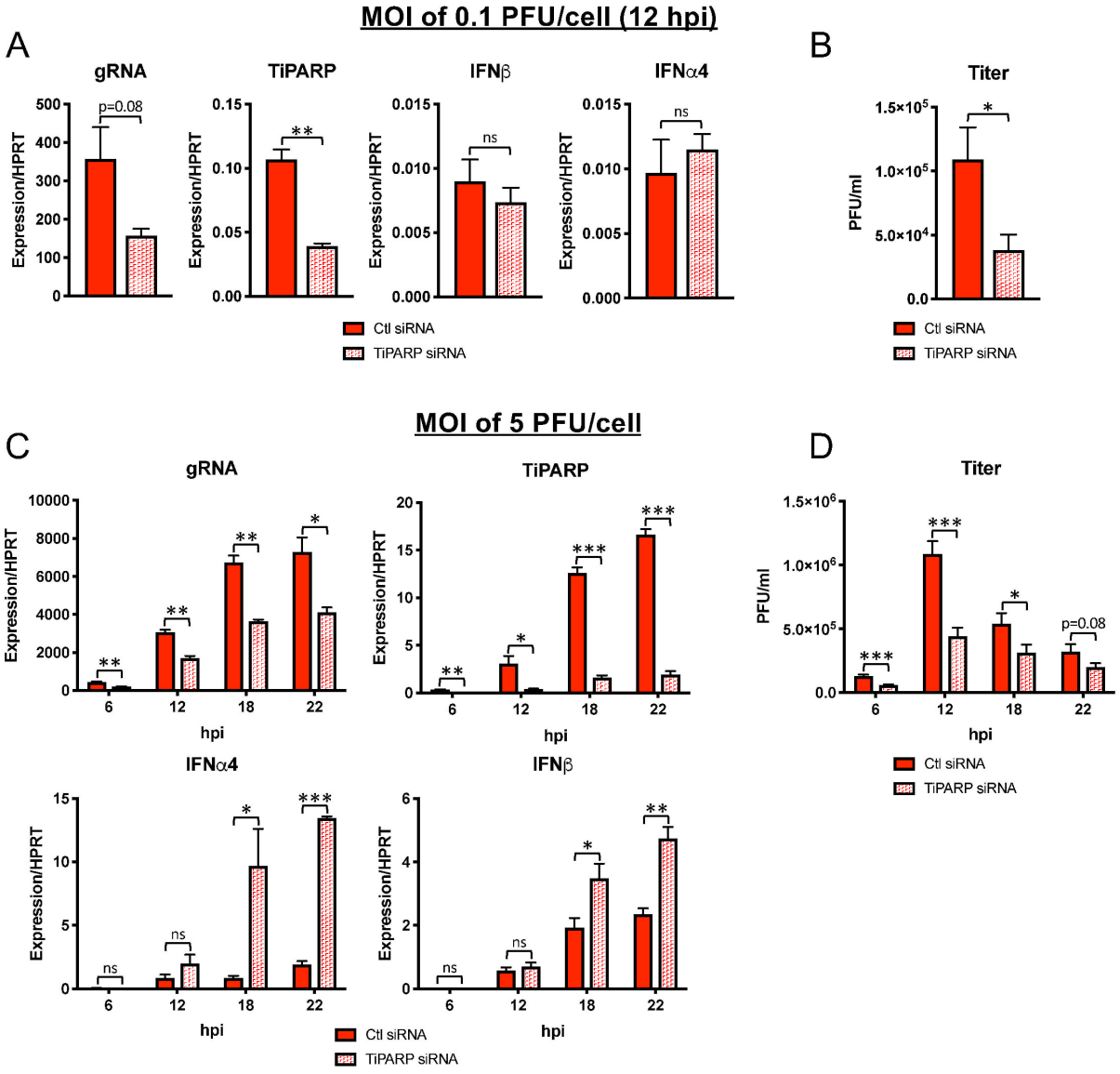

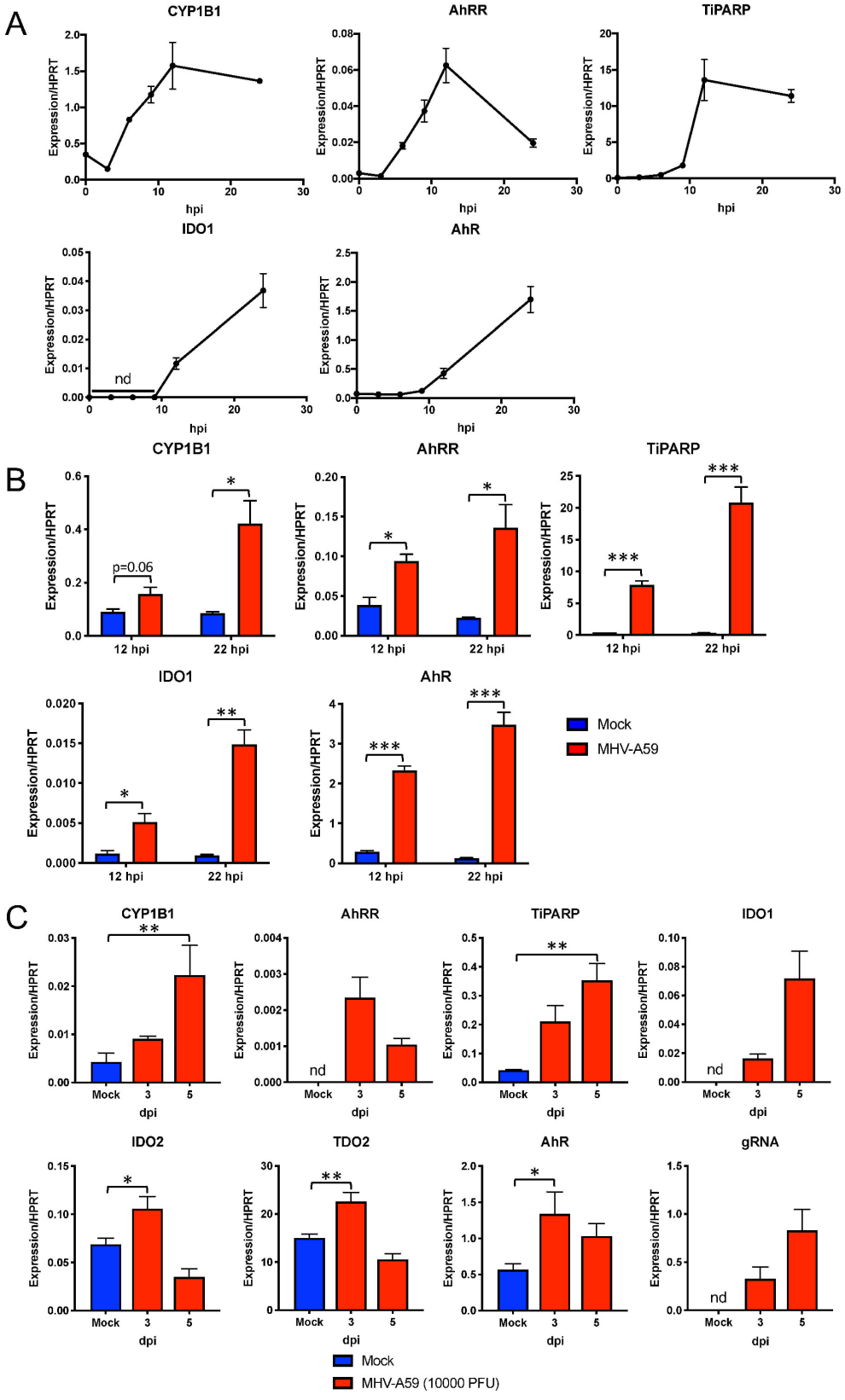

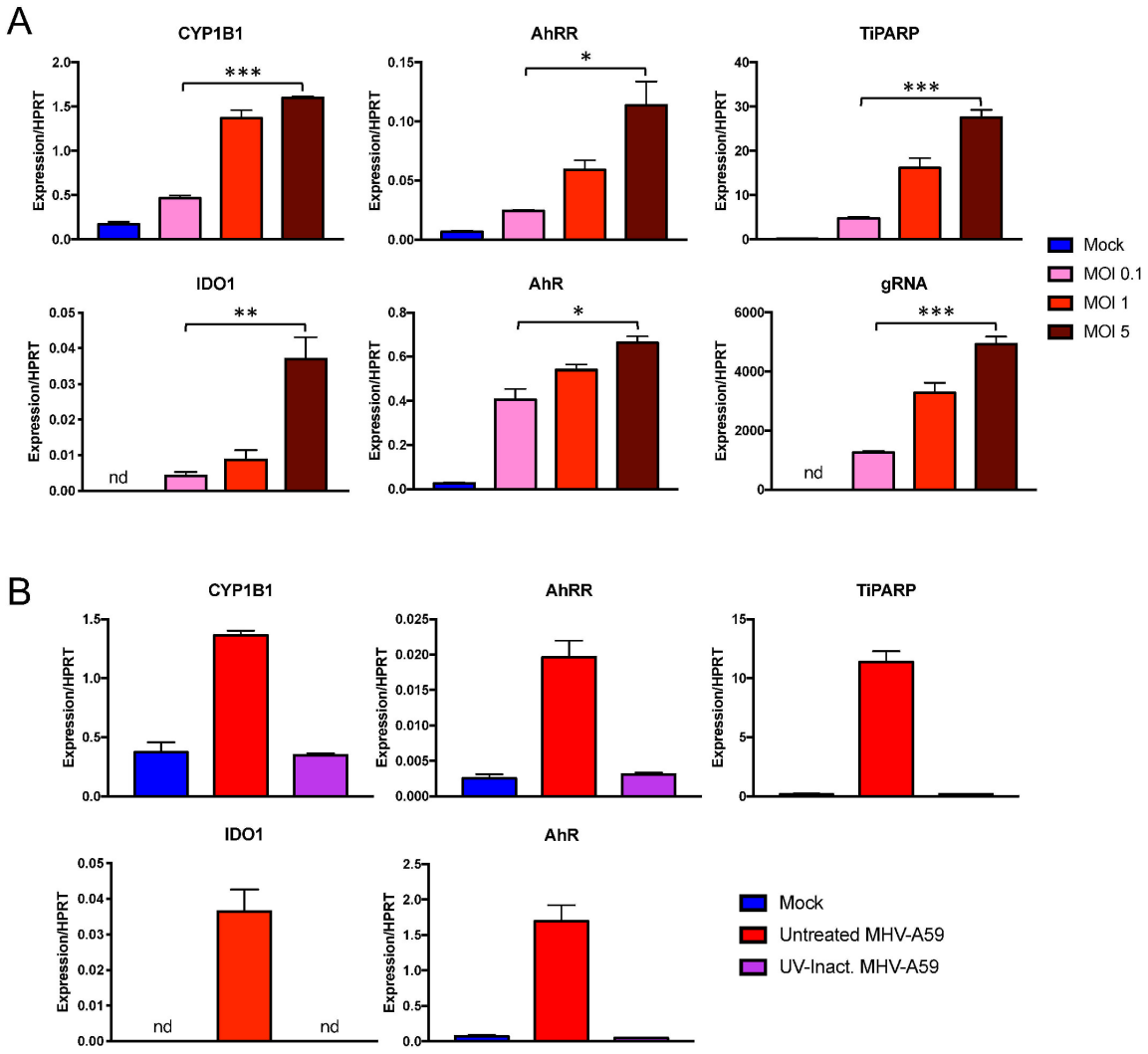

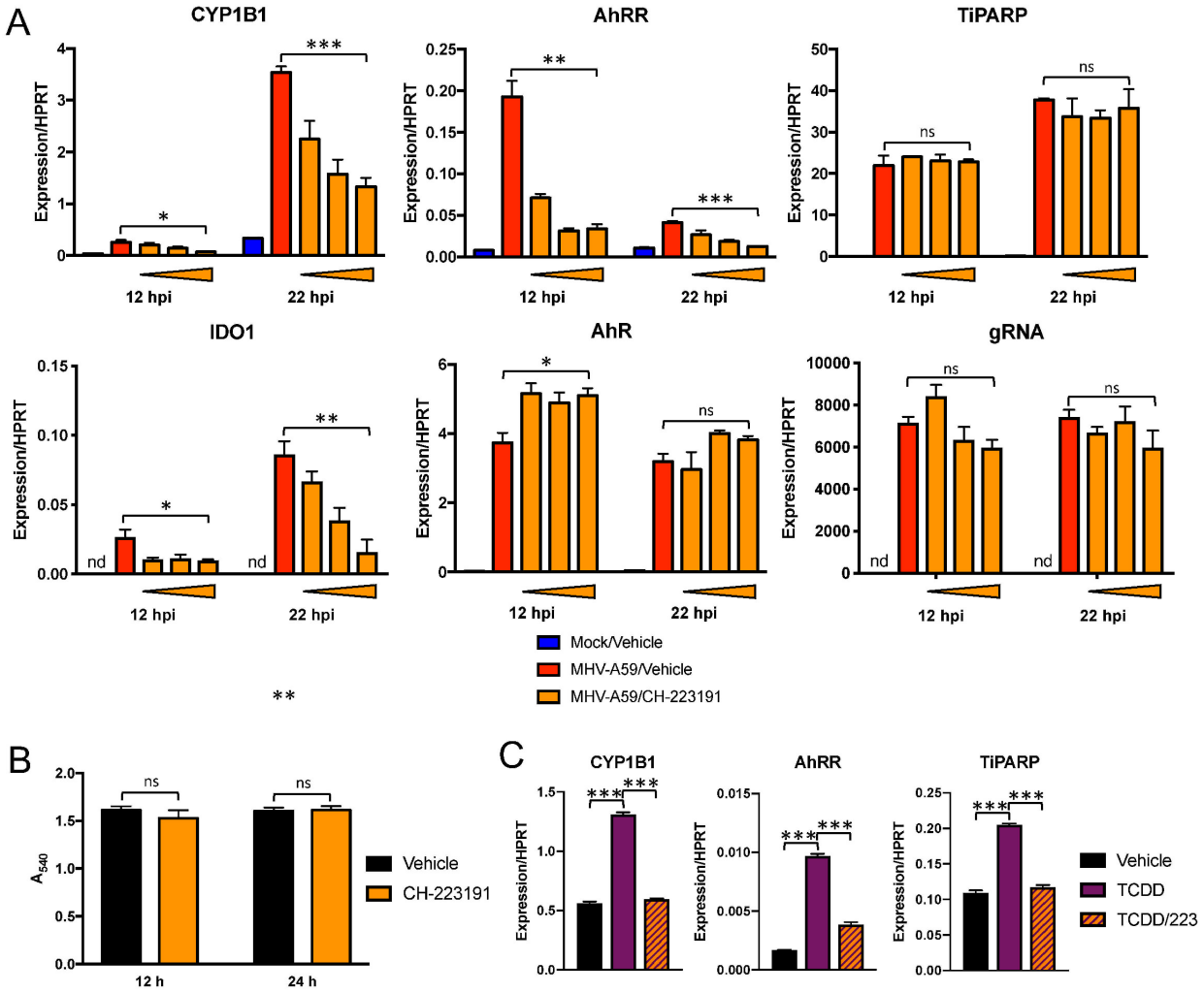

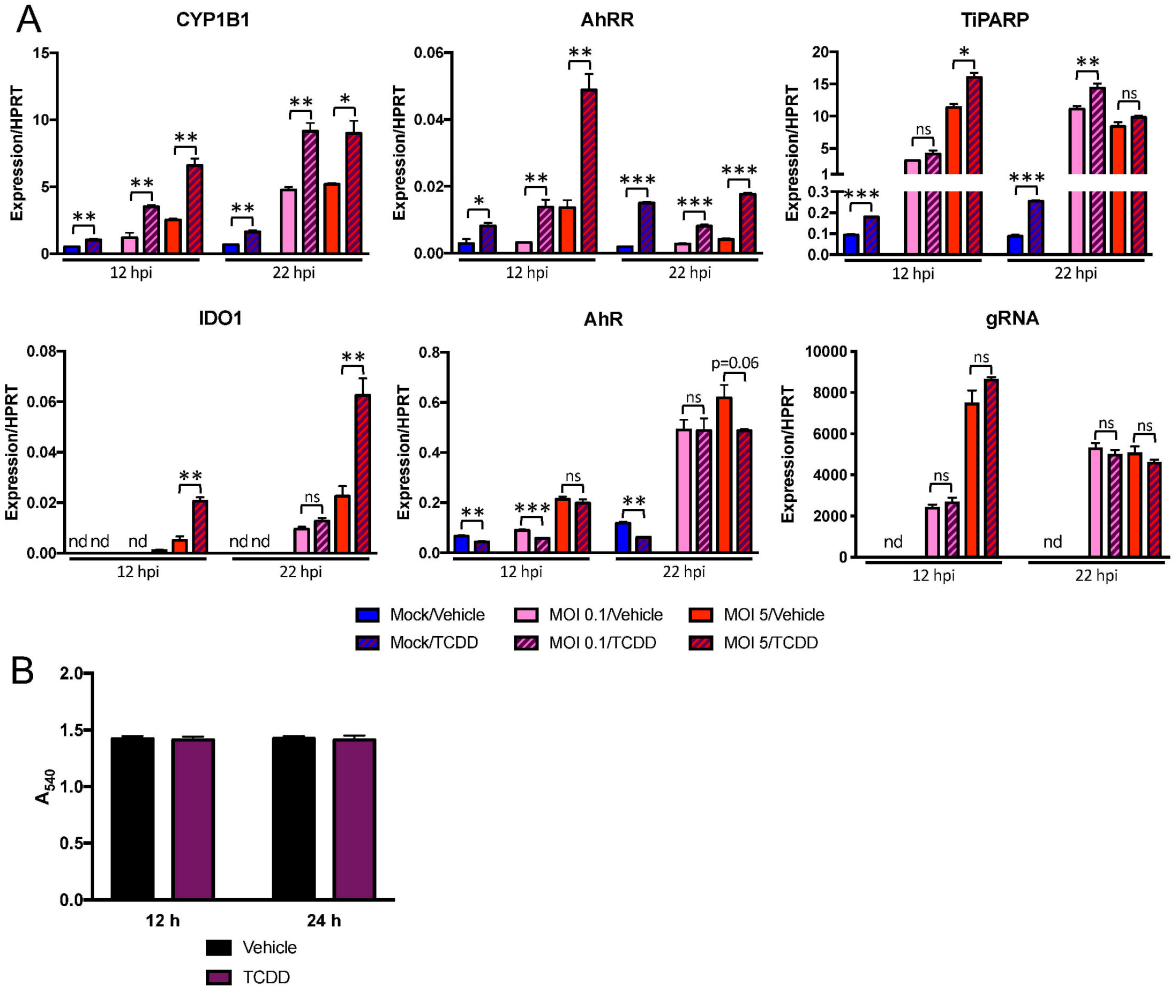

Journal of Virology

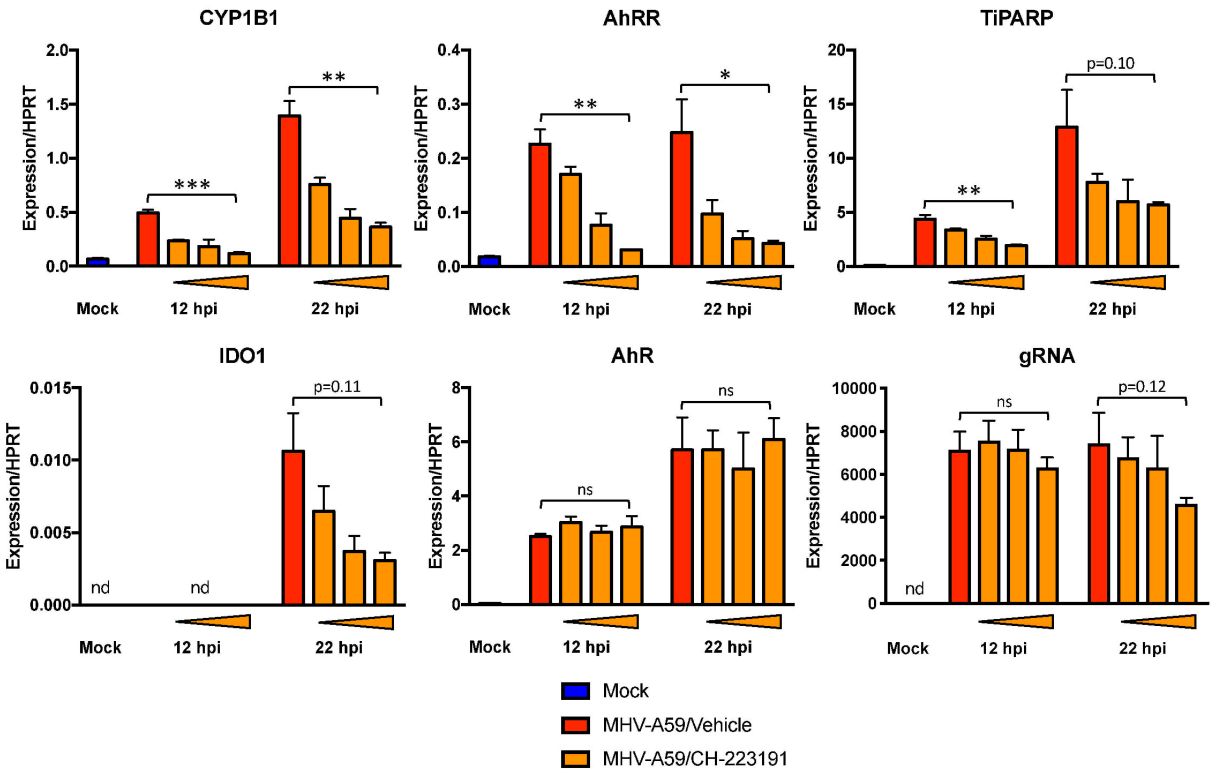

Journal of Virology

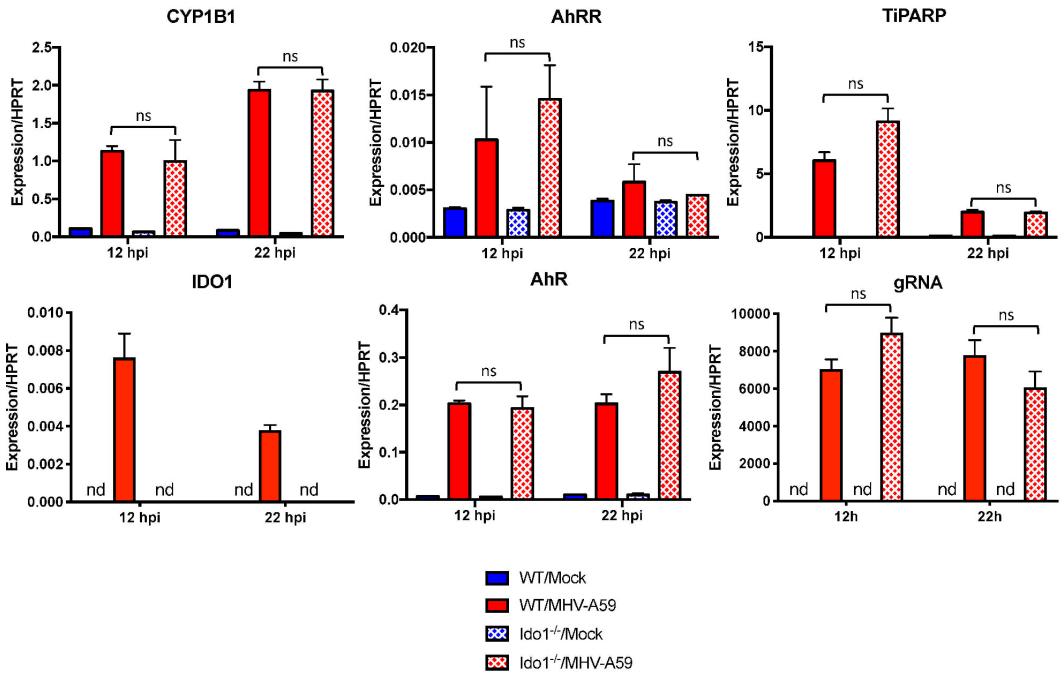

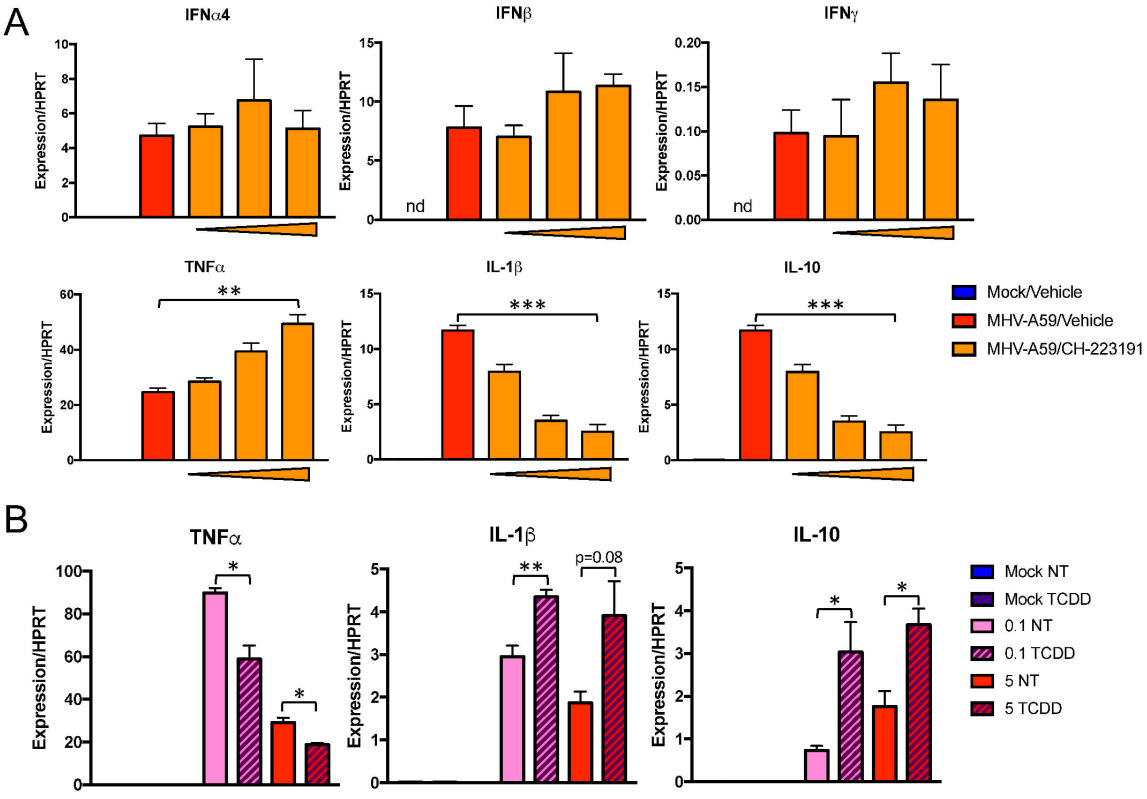

Journal of Virology